(Received 24 February 2026, Accepted 2 April 2026, Scheduled 23 April 2026)

Different Polygonal Clustered Subarray Partitioning Structures Synthesis with High Performance Beam Pattern

Randa Y. Hussein and Ahmed J. Abdulqader*

College of Electronics Engineering, Ninevah University, Mosul, Iraq

ABSTRACT: Synthesizing large arrays composed of irregularly clustered subarrays is a research approach that is attracting increasing attention from researchers. In this study, an irregular clustered subarray tiling strategy based on different polygonal shapes as masks and a convex optimization algorithm (COA) is proposed. A set of polygon partitions was proposed by formulating the problem of tiling an array of irregular subarrays to make it suitable for any aperture grid. To further reduce the complexity of the systems and accelerate the execution time of the corresponding algorithm, amplitude-only feeding was considered. In all the proposed partitioning scenarios, only 16 polygonal clusters (i.e., a complexity of 1.7%) were synthesized, achieving high-constraint radiation performance targets by reducing the sidelobe level (SLL) to -45 dB and generating a 6-degree wide and -180 dB deep null steering with the ability to orient the main beam as required. Polygonal clusters of varying sizes, shapes, and side counts were synthesized, ranging from a three-sided polygon (i.e., a triangle) to a ten-sided polygon (i.e., a decagon). Based on this, six polygonal segmentation configurations were proposed, resulting in a high-performance electromagnetic beam pattern (BP). Computer simulation results demonstrated the robustness and effectiveness of the proposed scenarios in meeting the performance constraints imposed on the optimization algorithm. The good performance and potential inherent in the methods presented in this study were verified by comparing them extensively with current methods in various numerical examples.

1. INTRODUCTION

Phased and non-phased antenna arrays have become widely used in many modern wireless applications, such as radar systems, particularly those with large elements, to achieve optimal electromagnetic performance. Increasing the number of radiating elements in an array significantly expands the radiation range of the antenna system and makes numerous contributions in terms of signal processing, such as signal steering and detection, removal of noise and interference signals, and the provision of spatial resolution. However, the practical handling of large array elements is not an easy task, because of the complexity of the transmission/reception system and the increased burden of optimization computing [1]. Several effective engineering methods have been proposed to solve these problems, most notably the synthesis of apertures by dividing them into subarrays to address the challenges [2]. This technique is based on shaping the electromagnetic beam at the subarray level at a much lower computational and systemic cost than at the level of individual elements. The synthesis of subarrays directly affects the performance of array signal optimization algorithms [3].

Several clustered subarray configurations have been used by designers, the most common of which are regular, irregular, and nested [4]. Synthesizing regular subarrays is one of the easiest techniques to implement; however, it suffers from unforgivable radiation problems owing to the generation of high and periodic side lobes [5]. This problem was solved by making the tuning irregular and distributing the feed centers of the clusters periodically across the aperture so that each cluster independently triggers a different response distribution in the antenna system. All synthesis algorithms and cluster formation methods applied to different array apertures suffered from the problem of reducing SLLs and generating null steering. This suffering revealed ambiguity in the directions of the electromagnetic signals affecting the array pattern. Therefore, if the direction of the interference signal matches one of these signals, the improved weights may also reduce the level of the main beam or generate a null steering in the main beam region, causing a large distortion in the generated beam pattern and thus a loss of the useful electromagnetic signal [6]. Therefore, researchers face two major challenges. The first challenge is synthesizing high-performance radiation subarrays, and the second challenge is forming a small number of efficient clusters without compromising radiation performance, thus facilitating operational maintenance and system adaptability. An example of addressing the second challenge is using symmetrical or similar rotated cluster subarrays to fill the desired array aperture [7].

In the literature, numerous optimization algorithms have been used to solidify the idea of synthesizing differently-shaped subarrays and producing the desired radiation patterns. These algorithms include evolutionary algorithms such as the genetic algorithm (GA) [8], particle swarm optimization (PSO) [9], etc., and mathematical algorithms such as COA [10], Compressed sensing [4], etc. In [11], finding the optimal solution for synthesizing an antenna array using a GA was considered. A problem arose in this study: it did not guarantee complete

* Corresponding author: Ahmed Jameel Abdulqader (ahmed.abdulqader@uoninevah.edu.iq).

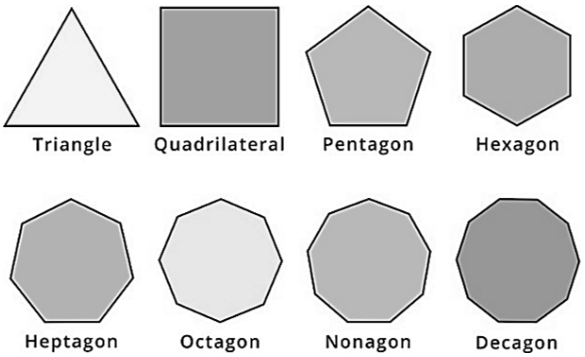

FIGURE 1. Different types of polygonal shapes.

coverage of the radiation performance, leaving some gaps in the result, which negatively impacted the array's efficiency in terms of directivity. In [12], an innovative Bayesian algorithm was proposed to solve the problem of constructing contiguous subarrays. Unfortunately, this method struggled to achieve robust, non-overlapping solutions in the array aperture. One of the difficult problems that arises in the synthesis of subarrays is the overlap of the structures of the formed clusters, which leads to a shortage of patterns in the final designs. To avoid this problem, the results in [13] showed an optimal combination by proposing domino-like clusters that provided complete coverage of the aperture without overlapping and offered the best radiation performance. Ref. [14] also addressed the X algorithm to achieve precise cover solutions in order to find precise structures for filling the array without overlapping. However, the problem was concentrated in the time taken and the high computational costs of the synthesis process. Moreover, finding the perfect clustered subarray synthesis within a huge solution space to achieve efficient and robust radiation performance is extremely difficult.

The designs of clustered subarray structures vary in their effects on the performance of the resulting beam pattern; therefore, it is necessary to choose suitable architectures to suppress the sidelobe levels significantly or to orient different null areas to prevent interference or distortion. It is preferable to tile subarrays that are spatially and dynamically adaptable in form, so that they take irregular and adaptively changing forms as required. Therefore, in this study, a synthesis of polygon-based dividing masks, compatible with a square array aperture, was proposed to generate regular and irregular clustered subarrays. The optimization task was assigned to the COA, owing to its high efficiency, particularly in subarray synthesis techniques. Amplitude-only feeding was used exclusively to excite polygon cluster elements and reduce systemic and computational complexity. The synthesis of six polygon-based segmentation mask architectures was proposed to improve the performance of highly constrained electromagnetic BP. The MATLAB tools' environment was used to implement all the proposed optimization scenarios.

2. POLYGONAL SUBARRAYS COVERING SYNTHESIS

To construct a cluster mask controller based on spatial division in the Cartesian axes, two types of partitioning covers are derived depending on the distribution of elements within the array aperture. The construction of two types of cover structures responds to the requirements of synthesizing regular and irregular subarrays innovatively. To synthesize polygonal cluster covers that emulate the shapes of the array apertures, the array parameters are first defined with equally spaced elements, thereby providing a fixed position for each element, and ensuring that the elements are contained by the generated clusters without overlaps. Based on this, two types of polygonal masks can be synthesized depending on which best covers the radiating elements. Therefore, different polygonal shapes can be considered for use as clusters within partition covering masks (see Figure 1).

2.1. Regular Polygonal Subarrays Covering (RPSC)

To place a regular covering mask consisting of polygonal geometric shapes with equal-length sides, a polygonal seed is generated and placed in one corner of the two-dimensional array. Subsequently, the entire covering mask is completed with several polygons similar in shape and size to the seed. To accomplish this, first, the dimensions of the array comprising $N \times M$ elements placed at equal distances on the two axes, x and y, are defined as follows:

$$x = d_x\left(n - \frac{N-1}{2}\right) \tag{1}$$

$$y = d_y\left(m - \frac{M-1}{2}\right) \tag{2}$$

These elements can be placed in a 2D matrix in the following order:

$$B_{ij} = \begin{bmatrix} x_1y_1 & . & . & x_iy_1 \\ . & . & . & . \\ . & . & . & . \\ x_1y_j & . & . & x_iy_j \end{bmatrix}, \quad \begin{matrix} i = 1, 2, \ldots, N \\ j = 1, 2, \ldots, M \end{matrix} \tag{3}$$

To formulate a mathematical model through which the polygonal cover is controlled so that the array aperture is divided into a set of specific and regular clusters, each polygonal area is defined by a set of the following mathematical parameters: c (center point), r (radius), and s (number of sides). These parameters determine the spatial distribution of each polygon within the main mask cover compatible with the dimensions of the 2D array. These parameters can be expressed mathematically as follows:

$$c_{xy} = \begin{bmatrix} c_{11} & . & . & c_{p1} \\ . & . & . & . \\ . & . & . & . \\ c_{1p} & . & . & c_{pp} \end{bmatrix}, \quad p = 1,\, 2, \ldots, P \tag{4}$$

where P is the number of polygons. Therefore, a polygon can be defined geometrically using these parameters:

$$\underbrace{P_{r,s}}_{x,y} = \begin{bmatrix} c_x + r\cos[\frac{2\pi}{T}s] \\ c_y + r\sin[\frac{2\pi}{T}s] \end{bmatrix},$$

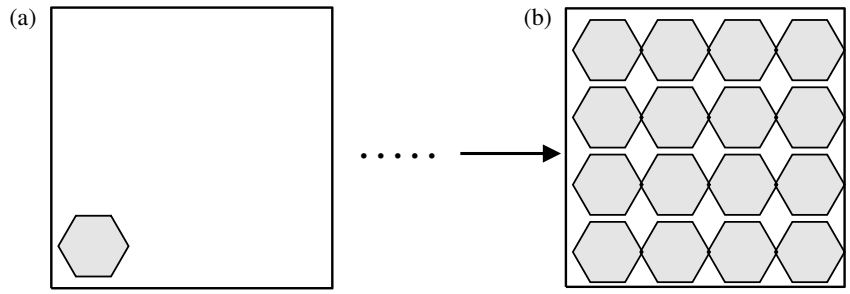

FIGURE 2. NRPC with $s = 6$ (hexagonal) structure. (a) Generating a single polygon cluster. (b) Generating 16 polygon clusters.

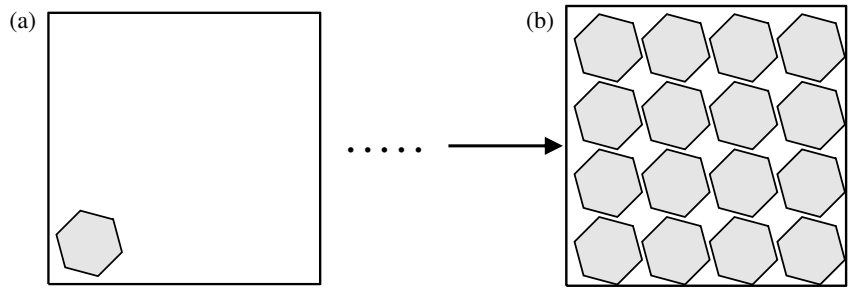

FIGURE 3. RRPC with $s = 6$ (hexagonal) rotated 45 deg. Counterclockwise structure. (a) Generating a single polygon cluster. (b) Generating 16 polygon clusters.

$$s = 3,\ 4, \ldots, total\ number\ of\ sides\ (T) \tag{5}$$

In this manner, polygonal shapes of different sizes and sides are combined to build a decorative covering mask composed of several similar polygonal shapes in order, with the possibility of rotating them and controlling their size. It is worth noting that increasing the number of sides of the polygon, $s > 15$, can transform the shape of the polygon into a circle within the imposed mask. Figures 2 and 3 show the possible configurations of regular polygons that are equal in size and number of sides, with the possibility of rotating them (for example, a 45° counterclockwise rotation). Two types of tiling configurations, non-rotated regular polygonal clusters (NRPC) and rotated regular polygonal clusters (RRPC) can be generated.

The arrangements shown in the two figures provide flexible modification to polygonal clusters in terms of size, shape, and rotation direction without affecting the coordinates of the basic array aperture. Now, the radiating elements in the array aperture were linked to the generated polygons by the proposed partition mask through a cluster joining experiment of the elements. Therefore, an indicator in the mask curtain $\xi_{i,p}$ is defined as follows:

$$\xi_{i,p} = \begin{cases} 1 & B_{ij} \in \underbrace{P_{r,s}(p)}_{x,y} \\ 0 & otherwise \end{cases} \tag{6}$$

This condition results in a definitive partitioning of the array elements based on spatial proximity and area coverage of the polygon. It is worth noting here that polygonal shapes may not extend fully within the applied mask curtain to the array, which may produce elements not intended for the resulting cluster. This problem can be solved by including some of these unallocated elements in the nearest polygon based on the principle of Euclidean spacing reduction and by excluding the other unallocated elements. In other words, including non-assigned elements to nearby polygons will be based on the following:

$$\overline{p_i} = \arg\min_{p} \|B_{ij} - c_{xy}\|_2 \tag{7}$$

where $\|.\|_2$ is norm2. Therefore, the clustered subarrays can be expressed as follows:

$$clustered\ subarray(i) = \overline{p_i} \tag{8}$$

2.2. Irregular Polygonal Subarrays Covering (IPSC)

In this section, to increase the ease of tiling clustered arrays, thereby affording later high flexibility and more degrees of freedom to the improved algorithm, different size and side polygons are tiled. This property enables better utilization of radiating elements in groups within the array aperture. Consequently, more irregular polygonal mask covering synthesis cases are generated. Additionally, the polygon rotation feature can be enabled to achieve more dynamic tiling configurations. Here, several factors must be considered when composing this type of cluster. For example, the number of clusters being tiled, the number of sides per polygon and the direction of their rotation provide many possibilities for tiling. There are two types of tiling, non-rotated irregular polygonal clusters (NIPC) and rotated irregular polygonal clusters (RIPC), as shown in Figures 4 and 5.

These covering cluster masks are characterized by parameters that directly affect the performance of the array aperture from an electromagnetic perspective, including the number of polygonal sides and their size (i.e., the area of coverage of the polygon as a cluster). To increase the flexibility of controlling the proposed RIPC-polygonal clusters, Figures 6 and 7 illustrate the generation of a polygonal mask network with varying

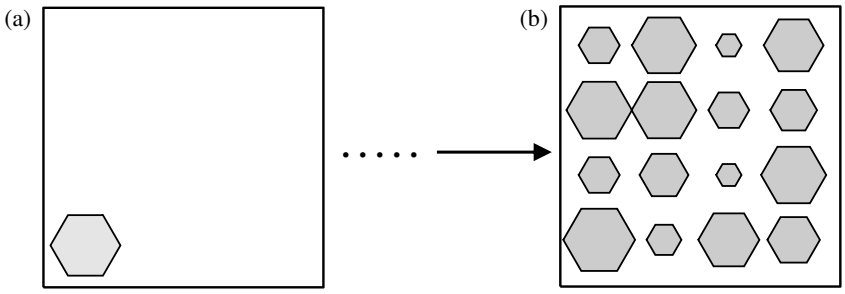

FIGURE 4. NIPC with $s = 6$ (hexagonal) structure. (a) Generating a single polygon cluster. (b) Generating 16 polygon clusters.

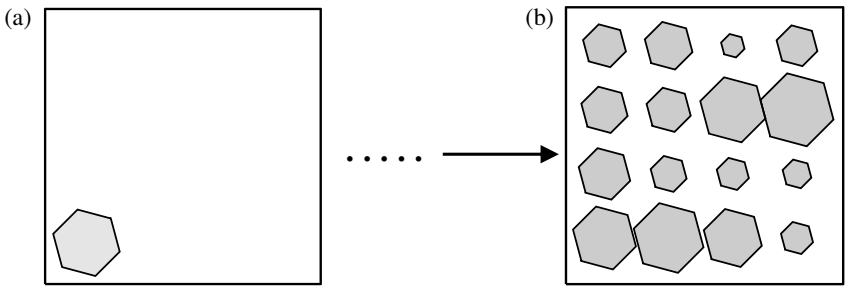

FIGURE 5. RIPC with $s = 6$ (hexagonal) rotated 45 deg. Counterclockwise structure. (a) Generating a single polygon cluster. (b) Generating 16 polygon clusters.

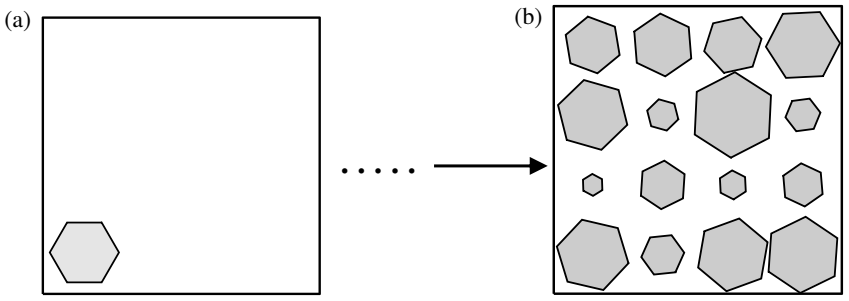

FIGURE 6. RIPC with different radii and rotation structures. (a) Generating a single polygon cluster. (b) Generating 16 polygon clusters.

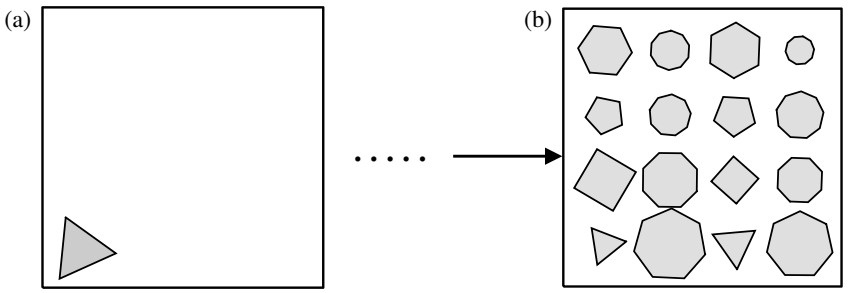

FIGURE 7. RIPC with different numbers of sides and rotation structures. (a) Generating a single polygon cluster. (b) Generating 16 polygon clusters.

sides and rotation angles. This flexibility may give the algorithm greater ease and probability of synthesizing patterns more efficiently than other methods.

2.3. Polygonal Clustered Subarray Elements Feeding

Consider a square array aperture consisting of $N \times M$ elements placed on the x and y axes as shown in Eqs. (1) and (2). This aperture possesses an array factor ($\mathbb{F}$), which contains several special optimization parameters for tuning a robust beam pattern, as illustrated in:

$$\mathbb{F}(\theta, \phi) = \sum_{n=1}^{N} \sum_{m=1}^{M} I_{nm} e^{-j\frac{2\pi}{\lambda}[x_n(\theta-\theta_o)+y_m(\phi-\phi_o)]} \quad (9)$$

where I_{nm} is the complex feeding comprising amplitude $|I_{nm}|$ and phase $\angle I_{nm}$, which is the target parameter in the subse-

quent optimization process. (θ, ϕ) are the basic orientation angles of the resulting beam, and in the default case, the orientation is at angle $(0, 0)$. To synthesize the feeding of elements to the formed clusters in the proposed polygonal covering masks, a set of elements is allocated to each cluster. Note that $|I_{nm}|$ it can only be optimized as an amplitude while keeping the phase $\angle I_{nm}$ zero for all elements to reduce the systemic and computational complexity. After a set of cluster masks for array partitioning has been generated and synthesized, the next step is to allocate the amplitude-only feeding to each cluster. To accomplish this, we establish a common link between the feeding for individual elements and clusters, as follows:

$$|I_{nm}| = |I_{p_i}| \quad for\ clustered\ subarray(i) = p \tag{10}$$

Therefore, the amplitude-only feeding of clustered elements can be expressed as follows:

$$|I_{p_i}| = [|I_1|, |I_2|, \ldots, |I_p|]' \tag{11}$$

A mathematical link is established in the form of a matrix between the radiating elements and the sub-cluster matrix, as follows:

$$E \in \{0, 1\}_{(N,M)\times p}, \quad E_{i,p} = \xi_{i,p} \tag{12}$$

Finally, the total number of elements is obtained as $|I_{nm}| = E|I_{pi}|$. Therefore, the array factor can be updated as:

$$\mathbb{F}(\theta, \phi) = \sum_{p=1}^{P} |I_{pi}| \sum_{n=1}^{N} \sum_{m=1}^{M} |I_{nm}| \, e^{-j\frac{2\pi}{\lambda}[x_n(\theta-\theta_o)+y_m(\phi-\phi_o)]} \tag{13}$$

Up to Eq. (13), the process of building clustered array structures is configured to optimize the beam pattern at the level of the cluster elements without compromising the physical accuracy of the array aperture.

With the proposed polygonal cluster masks, a set of constraints is imposed on the beam pattern to assess the effectiveness of the proposed scenarios. To ensure that the effectiveness of the presented methodology is not lost, the optimization task is assigned to the convex optimization model (COM) algorithm to efficiently improve the synthesis of amplitude-only triggers for cluster elements. This algorithm works by creating a compatible bridge relationship between the spatial partitioning of the array aperture based on different polygonal shapes and the amplitude excitation modeling of the resulting subarrays, thus providing a robust geometric design and formulation for developing the electromagnetic performance of the generated beam pattern. It is ambitious that polygonal masks support optimization tasks in terms of directing the main beam (if the phase excitation is activated), significantly reducing the SLLs, and generating a null steering to perfectly and completely cancel one of the sidelobes. These features are examined in the simulation results section. In addition to achieving these features, a clear and transparent mathematical model is provided for a perfect understanding of the optimization process and the ability to reproduce the desired results. The objective constraints imposed on the beam pattern are defined as follows:

$$E^H(\theta_o, \phi_o)\,|I_{pi}| = 1, \quad mean\ beam\ steering\ goal \tag{14}$$

$$\left|E^H(\theta_o, \phi_o)|I_{pi}|\right| \leq \beta, \ \forall(\theta, \phi) \in (\theta, \phi)_{SLL}\ exmpt(\theta_o, \phi_o) \tag{15}$$

$$SLLs\ reduction\ goal$$

$$E^H(\theta_{SL}, \phi_{SL})\,|I_{pi}| = 0, \quad null\ at\ any\ sidelobe\ angle \tag{16}$$

These constraints are combined into a single objective function to synthesize the desired beam pattern, as follows:

$$\begin{aligned} &\min_{|I_{pi}|} \left\|E^H(\theta, \phi)\right\|_\infty \\ &\quad S.t. \\ &\qquad E^H(\theta_o, \phi_o)\,|I_{pi}| = 1,\ and \\ &\qquad E^H(\theta_{SL}, \phi_{SL})\,|I_{pi}| = 0 \end{aligned} \tag{17}$$

Therefore, the optimization and synthesis processes for cluster polygonal covering masks can be summarized in Figure 8.

3. SIMULATION RESULTS

In order to demonstrate the effectiveness of the considered scenarios in synthesizing large array apertures, several structural tests were performed on a 2D array whose elements are $N \times M = 30 \times 30$. It is worth noting that the dimensions of the array can be changed to different dimensions, and the topology of the array can be changed to other grids, such as a rectangle, rhombus, circle, etc. The task of performing the synthesis of clustered arrays was assigned to the COA in all the presented scenarios, and the same optimization tools were installed. To make the computation easier, the amplitude-only feeding was considered, with the phase of all elements set to zero (if the main beam is not steered to a certain angle). In all structural scenarios, an attempt is made to obtain the radiation performance targets shown in Figure 9. These objectives include orienting the main beam at zero or other angles, reducing the SLLs to -45 dB or less, and generating a null steering at the angle 45° (with a width and depth of 6° and -180 dB, respectively). Also, in all the proposed structures, only 16 polygonal clusters are generated to cover the antenna aperture, taking into account a set of polygonal parameters in the optimization process, such as the shape and number of polygons, the number of sides, the size and radius of the polygon, and the angle of arrangement of the polygon. It is important to note that radiating elements near the polygonal mask are added to the cluster, while those farther away are considered inactive (i.e., in an off state). The results of the proposed scenarios will be reviewed in detail in the following sections.

3.1. RPSC Scenario Results

In this section, a clustered covering mask is generated from similar and non-rotated polygons based on the number of sides and size, with the following characteristics: $T = 6$ sides (hexagonal shape) and $r = 3\lambda$. To demonstrate how to achieve the performance targets shown in Figure 9, the method for reaching the desired beam pattern is presented, starting from the generation of the first cluster up to 16 clusters, as shown in Figure 10. It can be observed from this figure that the synthesis of one cluster does not perfectly meet the desired targets because of the high proportion of inactive radiating elements; however, with an increase in the number of clusters to three, it is observed that the beam pattern begins to approach the specifications of the objectives. Therefore, after the number of clusters is increased to

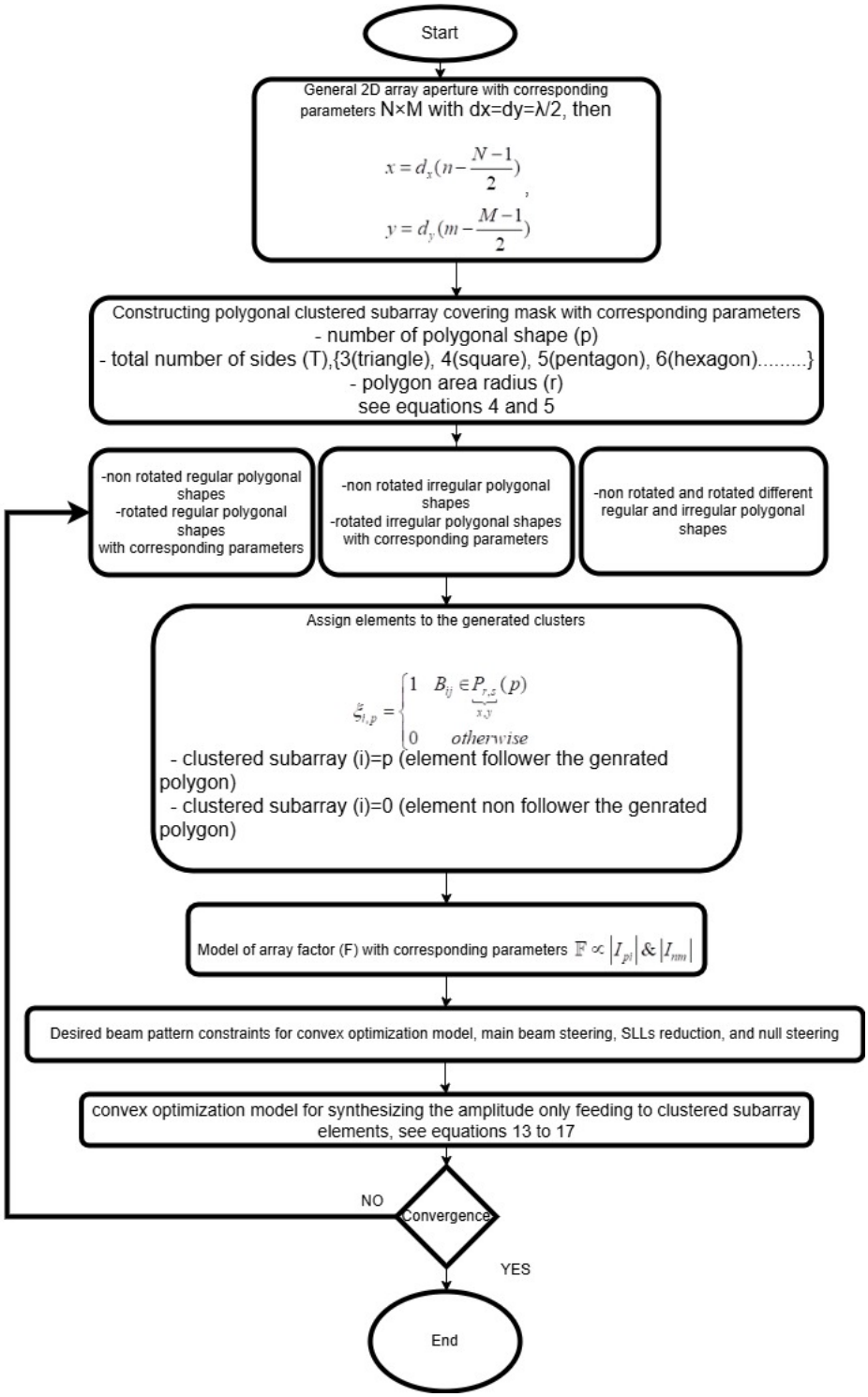

FIGURE 8. The flowchart of the optimization steps.

16, the targets are achieved better. In this method, because of the similarity of the generated clusters, it is observed that generating a wide and deep null is extremely difficult. All clusters, especially polygons with sides located inside the array aperture, take on the inclusion of some elements near their borders, which generates polygons as shown in Figure 10. This is part of the proposed plan to include as many radiating elements as possible in clusters to achieve the desired performance targets.

To increase the quality of performance targets, especially in terms of widening the null steering while also increasing its depth, all regular polygonal shapes are rotated at a 45-degree angle counterclockwise. This property resulted in a slight change in the shapes of the polygonal clusters, which provided a slight advantage to the algorithm leading to this positive change; consequently, the width of the null increased by two degrees (see Figure 11). It was worth noting that the reason

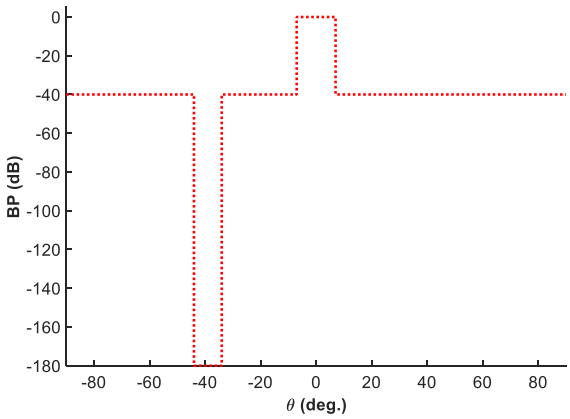

FIGURE 9. The radiation performance targets.

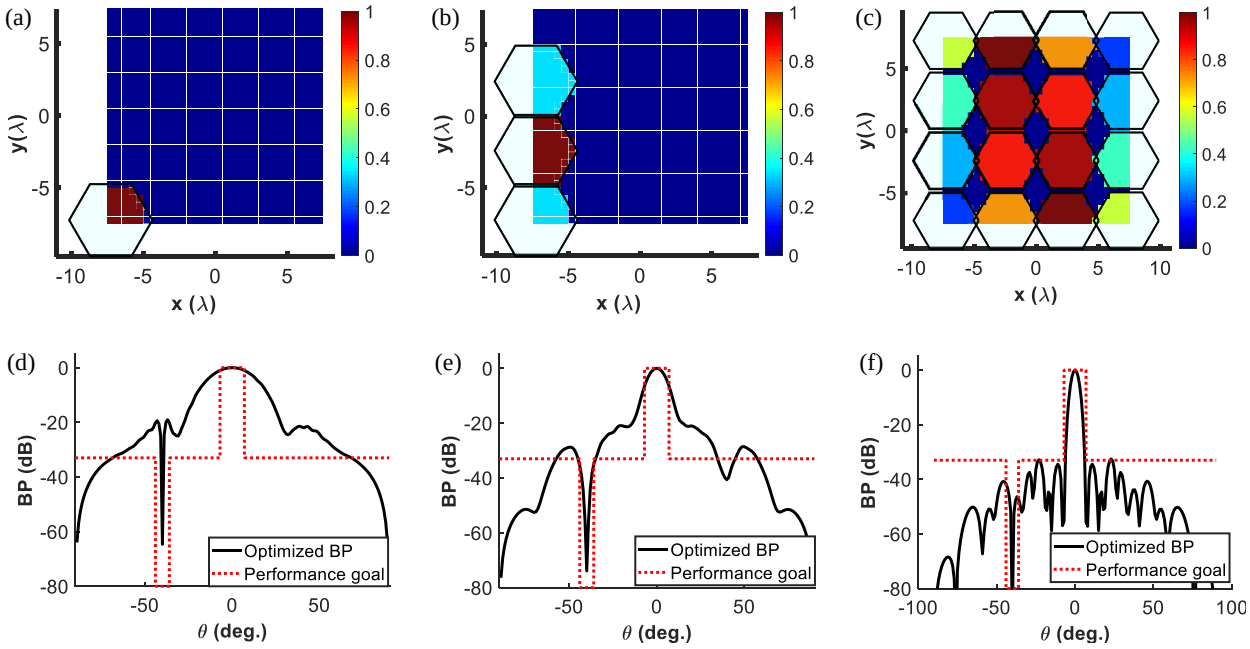

FIGURE 10. The NRPC results. (a) Generating a single polygon cluster with corresponding BP in (d). (b) Generating 3 polygon clusters with corresponding BP in (e). Generating 16 polygon clusters with corresponding BP in (f).

for the irregular arrangement of the SLLs at equal levels is the scattered distribution of amplitude-only feeding to the polygonal clusters after the optimization process. It is observed that the feeding of the maximum weights of the cluster elements was not concentrated in the middle of the aperture, but distributed in a scattered manner, which led to these results.

3.2. IPSC Scenario Results

In this section, a partition covering mask is constructed consisting of 16 hexagonal clusters ($s = 6$) with different radii. This combination provides more flexibility than the first scenario for the algorithm to achieve the performance goals. Figure 12 illustrates the results of this case. It can be observed from this figure that the main beam is maintained while reducing the SLLs by 3 dB, as well as maintaining the width and depth of the null steering as in Figure 9. Despite the overlapping polygonal shapes, the elements were assigned according to priority in generating these clusters, resulting in irregular and non-overlapping cluster elements. By adding the rotation property to the polygons, the quality of the desired radiation targets can be significantly increased. Figure 13 shows the results of the rotation property, where all polygons were rotated by an angle of 45 degrees counterclockwise.

It is evident from this configuration that the SLLs have been reduced to -40 dB while maintaining the fluctuation of the lobe levels close together and consistent owing to the concentration of the maximum weight feeding in the middle of the aperture, approximately. The depth of the null was also reduced to -180 dB while maintaining the main beam. In addition, the performance goals shown in Figure 9 can be achieved by combining other covering masks built with different angles of rotation polygons (see Figure 14) or by generating masks with a different number of sides and different polygon angles (see Figure 15).

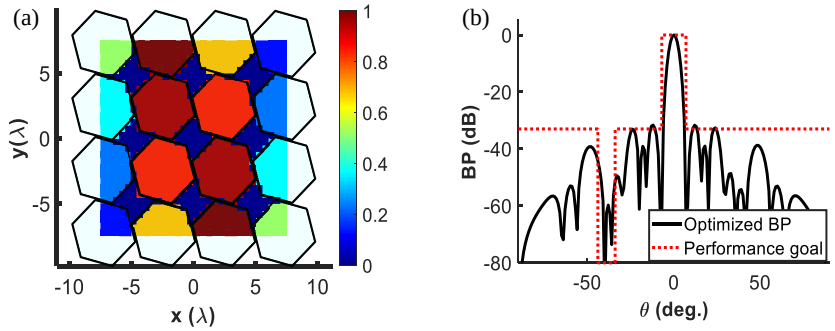

FIGURE 11. The RRPC with 45 deg. Counterclockwise rotation result. (a) Generating 16 polygon clusters with corresponding BP in (b).

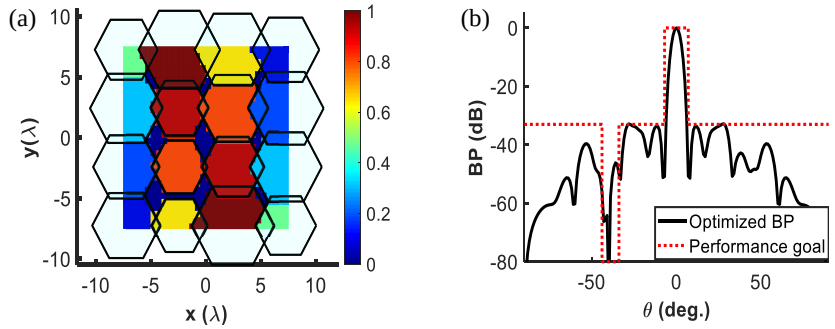

FIGURE 12. The NIPC with different radius results. (a) Generating 16 polygon clusters with correponding BP in (b).

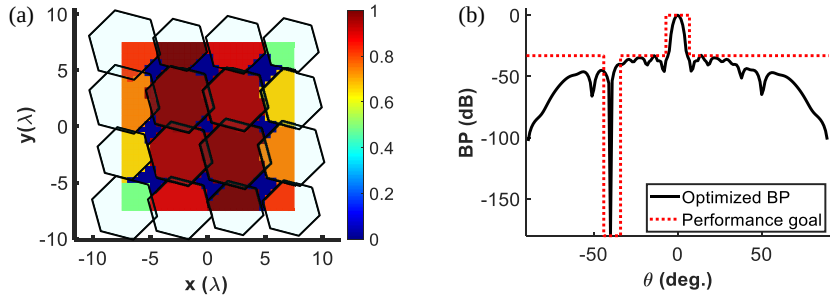

FIGURE 13. The NIPC with different radii and 45 deg. Counterclockwise rotation result. (a) Generating 16 polygon clusters with corresponding BP in (b).

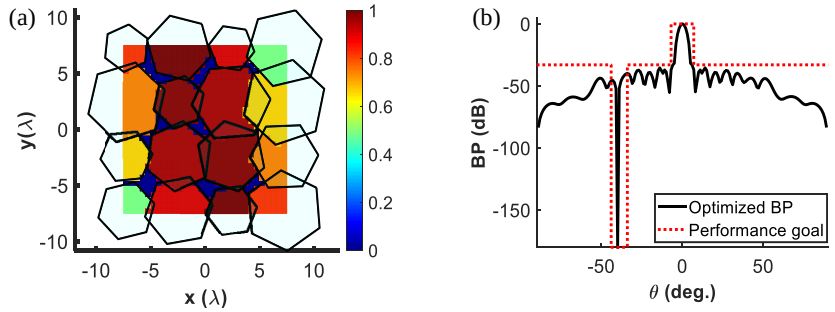

FIGURE 14. The RIPC with different radii and different rotation results. (a) Generating 16 polygon clusters with corresponding BP in (b).

In all the proposed mask covers, the overlap of polygonal shapes does not imply the overlap of elements between clusters. This depends on the priority of building the cluster and allocating its elements, as mentioned previously. Consequently, irregularly shaped subarrays were generated in most cases, confirming the theory of irregular tiling in enhancing the radial performance of the array pattern. Figures 16 and 17 illustrate the effect of polygonal cluster tiling structures on controlling electromagnetic performance targets, especially in terms of reducing the SLLs. Figure 16 shows the effect of the radius (r) of the

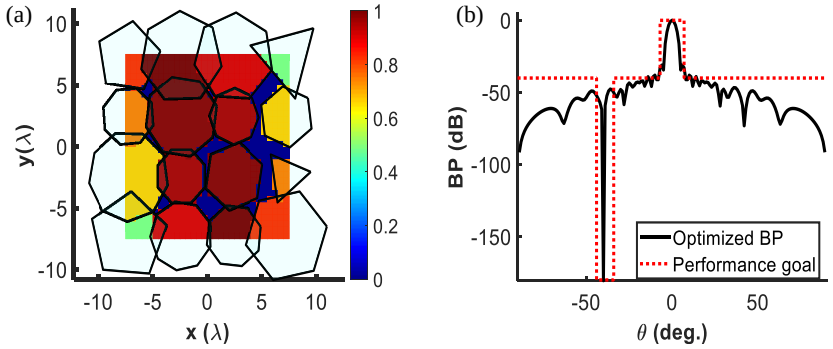

FIGURE 15. The RIPC with different numbers of sides and rotation results. (a) Generating 16 polygon clusters with corresponding BP in (b).

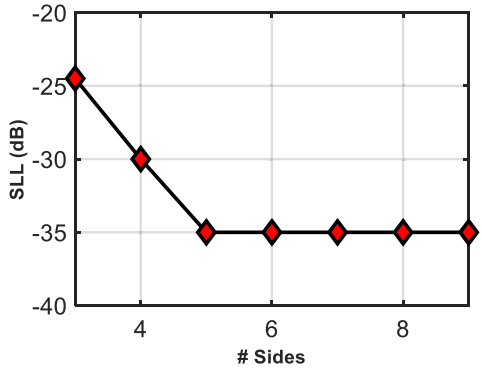

FIGURE 16. Variation of SLL output under different numbers of sides.

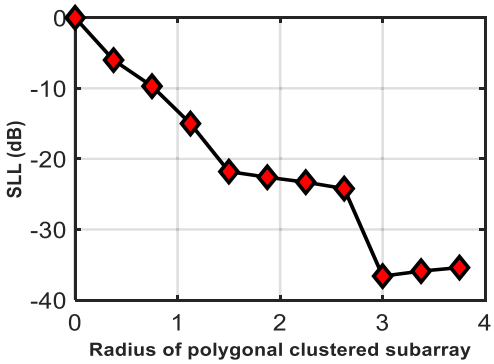

FIGURE 17. Variation of SLL output under different numbers of polygon radii.

polygon shape with a constant number of sides, and Figure 17 shows the effect of the number of sides (s) with a constant radius on controlling the SLLs.

As shown in Figure 16, by increasing the radius to a limit of 3.75λ while maintaining the number of sides constant at six (hexagonal shape), the SLL is reduced to -35.4 dB, with the highest reduction of -36.61 dB, obtained at a radius of 3λ. Increasing the polygon radius too much causes the generation of clusters with fewer than 16 elements owing to the large overlap between the clusters. Generating large polygons leads to the stacking of clusters on top of each other, thus prioritizing the initial clusters in allocating elements and reducing the number of subarrays to at most three or four. As shown in Figure 17, by increasing the number of sides (that is, changing the shape of a polygon from a triangle with $s = 3$ to a decagon with $s = 10$) while keeping the radius constant, the number of clusters is maintained at 16. This results in the synthesis of 16 different-shaped clusters, which enhances control over performance targets as required.

To examine the effectiveness of the results of the proposed scenarios in this paper and to compare them with the results of similar approaches achieved in previous literature, Table 1 presents an extensive comparative study. The table takes into account a comparison of a set of optimization parameters, including array aperture type, total number of radiating elements, total number of subarrays, feeding type (amplitude only, phase only, or both), complexity percentage, optimization method, and achievement of electromagnetic radiation performance goals in terms of beam steering, SLLs reduction, and null steering (width and depth). This comparison offers a well-defined design vision of important trade-offs that combine the robustness of the approach with the balanced adjustment of geometrically acceptable polygonal clusters. The results shown in [1–7] demonstrate that the approaches used deal with phased or complex feeding control of their cluster feeds with the synthesis of different types of array apertures in coordination with different types of optimization algorithms. This resulted in a set of acceptable improvements where the complexity percentage ranged from 3.6% to 16.7% and the SLLs from -13.1 dB to -29.8 dB, with the inclusion of the main beam steering feature in [1–3, 4–7] and the null steering feature in [2, 3]. As for Ref. [8], although the complexity percentage was greatly reduced to 1.75%, the achievement of performance goals was somewhat modest, as the SLL was reduced to -20 dB only, without achieving other goals. The use of a feeding system based on complex excitation has led to more advanced improvements than other systems, as described in [3] and [6]. The presented scenarios based on the COA offer highly superior radial and geometric performance in synthesizing a clustered polygonal square array aperture. This achieved the required performance targets with high professionalism, producing a reduction in the level of the sidelobes ranging from -35 dB to -45 dB and generating zero null orientation ranging from -80 dB to -180 dB, with the possibility of directing the main beam with high flexibility. In addition, all the synthetic scenarios achieved a high reduction in complexity percentage, reaching only 1.7%, which

TABLE 1. Details in performance of different approaches.

Ref.	Array type	# elements	# clusters	Feeding type	Complexity %	Optimization method	Performance goals			
							MBS (°) $(\theta, \emptyset)$	SLL (dB)	NS	
									Width (°)	Deep (dB)
[6]	Square	$64 * 64$	16	Phase only	3.9	Adaptive differential search	$(10, 0)$	-20	-	-
[4]	Circular	221	8	Phase only	3.6	CO	$(0, 0)$	-20	4	-50
[1]	Rectangular	$36 * 12$	8	complex	3.6	CO	$(20, 0)$	-24.5	4	-80
[15]	Square	$12 * 12$	12	complex	16.7	Improved Algorithm X	$(90, 20)$	-18	-	-
[16]	Rectangular	$22 * 12$	8	complex	6.06	L1 norm convex optimization	$(0, 0)$	-13.1	-	-
[17]	Linear	200	14	complex	7	Compressed sensing	$(0, 0)$	-29.8	-	-
[18]	Circular	349	8	complex	4.6	Heuristic iterative convex relaxation programming (H-ICRP)	$(20, 20)$	-15.206	-	-
[7]	Square	$20 * 20$	9	Amplitude only	1.75	GA	$(0, 0)$	-20	-	-
				Phase only	1.75	GA	$(0, 0)$	-20	-	-
Figure 10(c)	Square	$30 * 30$	16	Amplitude only	1.7	CO	$(0, 0)$	-35	4	-80
Figure 11(b)	Square	$30 * 30$	16	Amplitude only	1.7	CO	$(0, 0)$	-35	6	-80
Figure 12(b)	Square	$30 * 30$	16	Amplitude only	1.7	CO	$(0, 0)$	-35	6	-80
Figure 13(b)	Square	$30 * 30$	16	Amplitude only	1.7	CO	$(0, 0)$	-40	4	-180
Figure 14(b)	Square	$30 * 30$	16	Amplitude only	1.7	CO	$(0, 0)$	-40	4	-180
Figure 15(b)	Square	$30 * 30$	16	Amplitude only	1.7	CO	$(0, 0)$	-45	4	-180

makes these arrays practically simple to construct despite their large number of radiating elements. Due to the variety of scenarios, the IPSC architectures provided a significant reduction in the SLL, reaching -45 dB, with a 4° width and -180 dB depth. While structures (cases 3 and 4) achieved a reduction of -40 dB, the other structures achieved a reduction of -35 dB with zero null orientation, a width ranging from 4 to 6°, and a depth of -80 dB. In all proposed structures, the main beam was oriented towards 0°, with the possibility of orienting it to any desired angle. The current results demonstrate the robustness of using the COA in synthesizing polygonal clusters of different shapes and sizes, which ensures the required convergence and provides optimal control to achieve the proposed performance goals.

4. CONCLUSION

Efficient and robust innovative subarray optimization approaches based on the COA for synthesizing a square antenna array aperture are presented. Novel array partitioning methods are proposed based on generating different covering masks consisting of only 16 clusters in the form of regular and irregular polygons. A set of cluster polygons with varying sizes and numbers of sides is constructed to provide segmented coverage compatible with the array aperture dimensions, thereby producing efficient structures for generating highly restricted electromagnetic BPs. By relying solely on amplitude-only feeding and using only 16 clusters, the system complexity was reduced to only 1.7%. In addition to this advantage, robust

radiation characteristics were achieved, with a reduction in the SLL of −45 dB and the generation of broad and deep nulls of 6° and −180 dB, respectively, in some scenarios. Computer simulation results confirmed the validity of the proposed scenarios for synthesizing polygonal clusters and meeting the requirements of highly restricted BPs. Finally, the performance and capabilities of the approaches were verified by comparing them with similar techniques in the same field.

REFERENCES

[1] Dong, W., Z.-H. Xu, X.-H. Liu, L.-S.-B. Wang, and S.-P. Xiao, "Modular subarrayed phased-array design by means of iterative convex relaxation optimization," *IEEE Antennas and Wireless Propagation Letters*, Vol. 18, No. 3, 447–451, 2019.

[2] Chen, J.-Y., Z.-H. Xu, and S.-P. Xiao, "Optimal subarray design method for sidelobe cancellation of wideband irregular subarrayed array," *IEEE Antennas and Wireless Propagation Letters*, Vol. 22, No. 12, 2793–2797, 2023.

[3] Wang, X., E. Aboutanios, M. Trinkle, and M. G. Amin, "Reconfigurable adaptive array beamforming by antenna selection," *IEEE Transactions on Signal Processing*, Vol. 62, No. 9, 2385–2396, 2014.

[4] Elayaperumal, S. and K. V. S. Hari, "Optimal irregular subarray design for adaptive jammer suppression in phased array radar," in *2019 IEEE International Symposium on Phased Array System & Technology (PAST)*, 1–7, Waltham, MA, USA, 2019.

[5] Abdulqader, A. J., J. R. Mohammed, and Y. A. Ali, "A T-shaped polyomino subarray design method for controlling sidelobe level," *Progress In Electromagnetics Research C*, Vol. 126, 243–251, 2022.

[6] Pan, X., J. Chen, Z. Gu, and Z. Xu, "Wideband irregular subarrayed array structure optimization based on adaptive differential search for improved interference suppression," *IEEE Transactions on Aerospace and Electronic Systems*, Vol. 61, No. 5, 15 138–15 146, 2025.

[7] Abdulqader, A. J., "Low complexity irregular clusters tiling through quarter region rotational symmetry," *Progress In Electromagnetics Research C*, Vol. 137, 81–92, 2023.

[8] Gwee, B.-H. and M.-H. Lim, "Polyominoes tiling by a genetic algorithm," *Computational Optimization and Applications*, Vol. 6, No. 3, 273–291, 1996.

[9] Abdulqader, A. J., "Different 2D and 3D mask constraints synthesis for large array pattern shaping," *International Journal of Microwave and Wireless Technologies*, Vol. 16, No. 4, 579–587, 2024.

[10] Lebret, H. and S. Boyd, "Antenna array pattern synthesis via convex optimization," *IEEE Transactions on Signal Processing*, Vol. 45, No. 3, 526–532, 1997.

[11] Rocca, P., R. J. Mailloux, and G. Toso, "GA-based optimization of irregular subarray layouts for wideband phased arrays design," *IEEE Antennas and Wireless Propagation Letters*, Vol. 14, 131–134, 2015.

[12] Oliveri, G., M. Salucci, and A. Massa, "Synthesis of modular contiguously clustered linear arrays through a sparseness-regularized solver," *IEEE Transactions on Antennas and Propagation*, Vol. 64, No. 10, 4277–4287, 2016.

[13] Anselmi, N., P. Rocca, M. Salucci, and A. Massa, "Irregular phased array tiling by means of analytic schemata-driven optimization," *IEEE Transactions on Antennas and Propagation*, Vol. 65, No. 9, 4495–4510, 2017.

[14] Xiong, Z.-Y., Z.-H. Xu, S.-W. Chen, and S.-P. Xiao, "Subarray partition in array antenna based on the algorithm X," *IEEE Antennas and Wireless Propagation Letters*, Vol. 12, 906–909, 2013.

[15] Zhou, J., Y. Wang, Z. Wang, C. Pang, Y. Li, and X. Wang, "Irregular subarray tiling via rotational symmetry," *IEEE Antennas and Wireless Propagation Letters*, Vol. 22, No. 4, 903–907, 2023.

[16] Chen, J., Z.-H. Xu, and S. Xiao, "Irregular subarray design strategy based on weighted L1 norm iterative convex optimization," *IEEE Antennas and Wireless Propagation Letters*, Vol. 21, No. 2, 376–380, 2022.

[17] Zhao, X., Q. Yang, and Y. Zhang, "Synthesis of minimally subarrayed linear arrays via compressed sensing method," *IEEE Antennas and Wireless Propagation Letters*, Vol. 18, No. 3, 487–491, 2019.

[18] Dong, W., Z.-H. Xu, X.-H. Liu, L.-S.-B. Wang, and S.-P. Xiao, "Irregular subarray tiling via heuristic iterative convex relaxation programming," *IEEE Transactions on Antennas and Propagation*, Vol. 68, No. 4, 2842–2852, 2020.